PROTEIN STRUCTURE REPORT

The crystal structure of *Mycobacterium tuberculosis* adenylate kinase in complex with two molecules of ADP and Mg^{2+} supports an associative mechanism for phosphoryl transfer

MARCO BELLINZONI,[1] AHMED HAOUZ,[2] MARTIN GRAÑA,[1]
HÉLÈNE MUNIER-LEHMANN,[3] WILLIAM SHEPARD,[4] AND PEDRO M. ALZARI[1,2]

[1]Unité de Biochimie Structurale, [2]Plate-forme de Cristallogenèse et Diffraction des Rayons-X, [3]Unité de Chimie Organique, CNRS-URA 2185, Institut Pasteur, F-75724 Paris, France
[4]Synchrotron Soleil, L'Orme de Merisiers, Saint Aubin BP48, 91192 Gif sur Yvette, France

(RECEIVED February 15, 2006; FINAL REVISION February 15, 2006; ACCEPTED February 22, 2006)

Abstract

The crystal structure of *Mycobacterium tuberculosis* adenylate kinase (MtAK) in complex with two ADP molecules and Mg^{2+} has been determined at 1.9 Å resolution. Comparison with the solution structure of the enzyme, obtained in the absence of substrates, shows significant conformational changes of the LID and NMP-binding domains upon substrate binding. The ternary complex represents the state of the enzyme at the start of the backward reaction (ATP synthesis). The structure is consistent with a direct nucleophilic attack of a terminal oxygen from the acceptor ADP molecule on the β-phosphate from the donor substrate, and both the geometry and the distribution of positive charge in the active site support the hypothesis of an associative mechanism for phosphoryl transfer.

Keywords: adenylate kinase; phosphoryl transfer; X-ray crystallography; associative mechanism; *Mycobacterium tuberculosis*

Tuberculosis is a major world health problem, with one third of the total world population currently infected with *Mycobacterium tuberculosis* and more than two-million people dying annually from the disease. Sparked by the development of mycobacterial genomics (Cole et al. 1998), many efforts have been invested during the last few years in the identification and characterization of novel drug targets (Sharma et al. 2004; Andries et al. 2005). Among these, nucleoside monophosphate kinases (NMPKs) are of particular interest since they play a key role in the mainteinance of intracellular nucleotide pools in all living organisms.

Adenylate kinase (ATP:AMP phosphotransferase, EC 2.7.4.3; AK) is a ubiquitous enzyme which catalyzes the reversible, Mg^{2+}-dependent transfer of the terminal phosphate group from ATP to AMP, releasing two molecules of ADP. A large number of biochemical and structural studies have been conducted on AKs from different sources (Yan and Tsai 1999), and several crystal structures of the enzyme have been reported, both in the unligated form as well as in complex with substrates (ATP, ADP, and AMP) or substrate analogs (AMP–PNP or diphosphoadenosine-pentaphosphate, Ap5A). These studies reveal a conserved globular architecture composed of a central core made by a parallel β-sheet surrounded by α-helices, and a P-loop

Reprint requests to: Pedro M. Alzari, Unité de Biochimie Structurale, Institut Pasteur, 25 rue du Dr. Roux, F-75724 Paris Cedex 15, France; e-mail: alzari@pasteur.fr; fax: +33-1-45688604.

Article published online ahead of print. Article and publication date are at http://www.proteinscience.org/cgi/doi/10.1110/ps.062163406.

Table 1. *Diffraction data collection and refinement statistics*

Data collection	
Resolution[a] (Å)	31.37–1.9 (2–1.9)
Unique reflections	13,286
Multiplicity[a]	3.6 (2.7)
Completeness[a] (%)	95.8 (78.3)
R_{meas}[a,b]	0.086 (0.344)
Refinement	
Used reflections[c]	12,616
R-factor[d]	0.169
Free *R*-factor[d]	0.214
No. of refined atoms	
Protein	1452
ADP	53
RMS deviations	
Bond lengths (Å)	0.015
Bond angles (°)	1.65

[a] Numbers in parentheses correspond to the highest resolution shell.
[b] $R_{meas} = \{\sum_h (\sqrt{\{n_h/(n_h-1)\}}) \sum_j |\hat{I}_h - I_{h,j}|\}/\sum_{h,j} I_{h,j}$, where $\hat{I}_h = (\sum_j I_{h,j})/n_h$ and n_h is the multiplicity of reflection h.
[c] Five percent of reflections were left aside for calculation of free *R*-factor.
[d] R-factor $= \sum_{hkl} \|F_o| - k|F_c\|/\sum_{hkl} |F_o|$; R_{free}: same for the test set (5% of the data).

motif at the N terminus that binds the phosphoryl donor (ATP). Two regions of the protein, the LID and NMP-binding regions, participate in the isolation of the substrates during catalysis and usually undergo significant conformational changes during the reaction (Yan and Tsai 1999). The AK family can be classified into two groups on the basis of their polypeptide chain length, with the long variants possessing a longer LID domain as a consequence of a 25–40-residue insert. Eukaryotic cytosolic enzymes are of the short type, while mitochondrial, yeast, and bacterial AKs generally belong to the long type. Some bacterial AKs, including the *M. tuberculosis* enzyme, are actually short variants with limited sequence similarity to the eukaryotic cytosolic counterparts, and have been proposed to belong to a new group of short bacterial AKs (Munier-Lehmann et al. 1999).

In *M. tuberculosis,* AK is codified by the gene *adk* (Rv0733), and is composed of 181 amino acids. The recombinant enzyme expressed in *Escherichia coli* has been biochemically characterized (Munier-Lehmann et al. 1999), and its 3D structure in the absence of substrates has been determined by NMR methods (Miron et al. 2004). Here we describe the crystal structure of *M. tuberculosis* adenylate kinase (MtAK) at 1.9 Å in complex with two molecules of ADP and Mg^{2+}. The structure reveals significant conformational changes upon substrate binding and sheds light on the mechanism of the backward reaction. Despite the large number of available crystal structures of AKs (and those of closely related NMPKs) from different sources, no direct structural information has been reported for the ternary complex of the enzyme at the start of the backward reaction. Only the structure of uridylate kinase from *Saccharomyces cerevisiae* has been reported in complex with two ADP molecules (Muller-Dieckmann and Schulz 1995), but without the necessary Mg^{2+} ion.

Results and Discussion

Overall structure

The crystal structure of MtAK was determined at 1.9 Å resolution by molecular replacement methods using the structure of *Bacillus stearothermophilus* AK (Berry and Phillips 1998; PDB entry 1ZIP) as the search probe. A summary of data collection and refinement statistics is reported in Table 1. The overall structure is very similar to those of other AKs, displaying an LID region that is reduced to a 10-residue loop (Lys125 to Asp134) as in the eukaryotic cytosolic isoforms (Fig. 1).

It is well established that AK undergoes significant conformational changes upon substrate binding (Yan and Tsai 1999). In the case of MtAK, the solution structure (without ligands) shows the protein in a relatively closed conformation, similar to that found for the *E. coli* enzyme in complex with Ap5A (Miron et al. 2004), suggesting a possible explanation for its reduced catalytic activity. However, the structural superposition of the NMR and crystal structures reveals significant conformational rearrangements of MtAK upon substrate binding. The overall root-mean-squares deviation (RMSD) is 3.0 Å for all 181 Cα positions (1.7 Å for 122 core residues). As shown in Figure 1, however, residues from the NMP-binding domain (Thr31–Val59) show an RMSD of 3.6 Å, and those from the LID

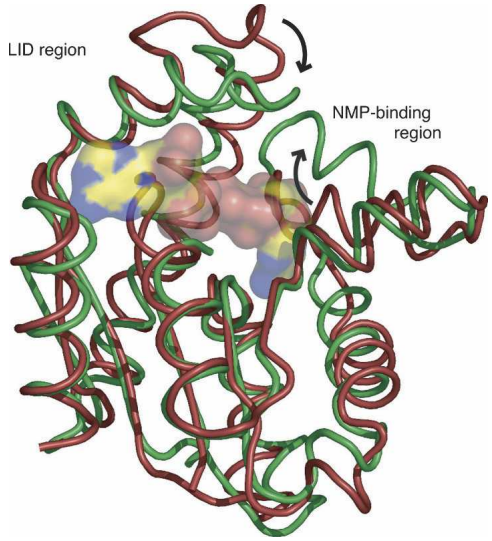

Figure 1. Superposition of the NMR structure of MtAK (Miron et al. 2004; PDB code 1P4S) in red, with the crystal structure of MtAK in complex with two molecules of ADP and Mg^{2+} (this work) in green. The ADP molecules are shown in transparent molecular surface representation. Significant movements of the LID and NMP-binding regions are indicated by arrows.

region (Lys125–Asp134) reveal a still larger rearrangement (6.4 Å), in agreement with the notion that the LID and AMP-binding regions undergo large conformational rearrangements during the catalytic cycle (Gerstein et al. 1993).

Protein–ligand interactions

In the crystal structure, a molecule of ADP binds to the ATP-binding site, while the NMP-binding site hosts either ADP or AMP with similar (50%) occupancy (Fig. 2A). An Mg^{2+} ion is also positioned at the center of the cleft, between the β-phosphates of each ADP ligand. The structure therefore represents the enzyme–substrate ternary complex immediately before the backward reaction, which leads to the phosphorylation of the ADP molecule in the ATP site, and the formation of AMP in the NMP site. As observed in other AK structures, the adenosine moiety of ADP in the ATP site interacts with the enzyme through a single hydrogen bond between the exocyclic amino group of adenine and the carbonyl oxygen of Gly166 (Fig. 2B), in agreement with the relatively poor specifity of AKs toward the nucleotide occupying this site. On the other hand, the adenosine moiety at the NMP site makes several hydrogen bonding interactions with protein residues (Thr31, Val59, Gly85, and Gln92; Fig. 2B). In particular, the carboxamide side chain of Gln92, which is hydrogen-bonded to the backbone amide of Arg88 and the hydroxyl group of Ser61, is equivalent to Gln101 in eukaryotic AK1, whose role in the discrimination of the NMP substrate has already been demonstrated by site-directed mutagenesis (Yan and Tsai 1999).

The ADP phosphate groups participate in an extended network of interactions. The conserved P-loop is fully closed over the ADP molecule in the ATP site (i.e., the acceptor substrate in the backward reaction), with all its phosphate oxygen atoms making hydrogen bonding interactions with backbone amide groups of P-loop residues Gly10, Gly12, Lys13, Gly14, and Thr15 (Fig. 2B). Moreover, the ε-amino group of Lys13 (the invariant lysine of the P-loop) is hydrogen bonded to the terminal oxygens of both ADP molecules. In contrast, the phosphate moiety of ADP from the NMP site interacts with the guanidinium groups of five arginine residues: Arg36 and Arg88 are hydrogen-bonded to α-phosphate oxygens, and Arg127, Arg129, and Arg140 to β-phosphate oxygens (Fig. 2B). The conserved Arg88 is a critical residue in the *E. coli*

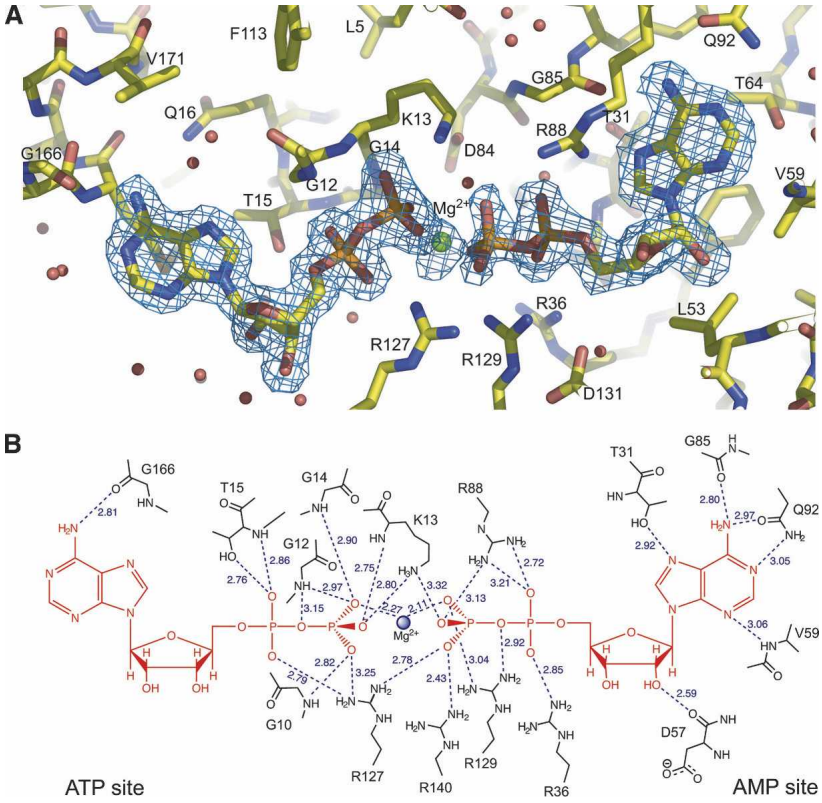

Figure 2. MtAK–substrate interactions. Panel *A* shows a close view of the substrate-binding cleft. The $2F_o - F_c$ electron density map at 1.9 Å resolution (contoured at 1 σ) is shown for the nucleotide substrates and the cofactor Mg^{2+} (green sphere). Water molecules are drawn as red spheres. Panel *B* shows a schematic representation of enzyme–substrate hydrogen bonding interactions (dashed lines), with the interatomic distances given in angstroms.

enzyme, where the R88G mutation lowers the activity of the backward reaction to 0.1% of the wild type, and leads to a 85-fold higher K_m value for AMP (Reinstein et al. 1989).

Although part of the LID loop, Arg129 interacts with the ADP bound in the NMP site (Fig. 2). This observation is consistent with the recent finding that the equivalent residue (Arg156) in the *E. coli* enzyme binds the AMP phosphate (Berry et al. 2006), and not the terminal phosphate of ATP as inferred from the previously reported structure of *E. coli* AK in complex with AMP and AMP-PNP (Berry et al. 1994). The above observations suggest that, in the *M. tuberculosis* enzyme, Arg129 may trigger the closure of the LID loop upon nucleotide binding to the NMP site, as proposed for the *E. coli* (Berry et al. 2006) and the *Methanococcus voltae* (Criswell et al. 2003) enzymes. It is worth noting that these observations are in contrast with the currently accepted view of an iso-random bi-bi mechanism for adenylate kinases (Sheng et al. 1999), which would require independent motions of the LID and NMP-binding regions.

The Mg^{2+} ion is in contact with the β-phosphates from both ADP substrates. The divalent ion is coordinated by the O2B oxygen atoms belonging to each β-phosphate, forming a bidentate complex, and two water molecules (Fig. 2). One of these water molecules interacts with the carboxylic oxygens of Asp84, another strictly conserved residue known to be necessary for Mg^{2+} binding (Rose et al. 1991), and with two terminal oxygens from the β-phosphate of the donor ADP. The second water molecule is positioned within hydrogen bonding distance to the hydroxyl group of Ser30 and to the guanidinium group of Arg36, which is also involved in fixing the α-phosphate of the donor ADP.

Catalytic mechanism

In the crystal structure, one terminal oxygen of the acceptor ADP directly points to the phosphorus atom of the donor β-phosphate, at a distance of 3 Å and in line with the P_β–$O_{\alpha,\beta}$ bond (Fig. 2A). The distance between the two P_β atoms is 4 Å, a shorter value than the medium range of 4.5–5 Å calculated in a recent molecular dynamics simulation of the *E. coli* AK in complex with ATP, AMP, and Mg^{2+} (Krishnamurthy et al. 2005). This geometry strongly suggests a direct nucleophilic attack of O1B on the P_β atom of the donor substrate, following an associative mechanism for the reaction. The distribution of positive charges in the active site further supports this model. In particular, the side chains of Arg127 and Arg140 bind the O3B oxygen of the transferable phosphate from opposite sides, and together with the ε-amino group of Lys13 and the Mg^{2+} ion, are well positioned to neutralize the negative charge developed on the trigonal bipyramidal transition state (Reinstein et al. 1990). Moreover, Arg129 makes a hydrogen bond with the α−β bridging oxygen of the donor ADP; this interaction, although compatible with a dissociative mechanism, may also be required for an associative mechanism to enhance the positive polarization of the phosphorus atom to be transferred, facilitating the nucleophilic attack by the incoming oxygen. A similar role has been proposed for the equivalent Arg93 in *Dictyostelium discoideum* UMP/CMP kinase (Schlichting and Reinstein 1997). It is worth noting that Arg127, Arg129, and Arg140 of the *M. tuberculosis* enzyme correspond respectively to Arg132, Arg138, and Arg149 in the *E. coli* enzyme, whose important role for the stabilization of the transition state has been demonstrated by mutagenesis (Yan and Tsai 1999).

Materials and methods

Protein production

The gene *adk* from *M. tuberculosis* was cloned into the expression vector pET-28a (Novagen). The recombinant plasmid was introduced in *E. coli* BL21(DE3) *pLysS* (Novagen) and the tranformed strain was grown at 30°C in LB medium containing 50 μg/mL kanamycin and 30 μg/mL chloramphenicol until the value of $A_{600} = 2.0$ was reached. Expression of MtAK was induced by adding 1 mM IPTG (isopropyl-thio-β-D-galactopiranoside), and the heterologous protein was purified as described (Munier-Lehmann et al. 1999).

Crystallization and data collection

The native protein was crystallized using the hanging drop vapor diffusion method by mixing 1.5 μL of protein solution (18 mg/mL) containing 5 mM AMP and 5 mM ADP with 1.5 μL of the reservoir solution containing 20% (w/v) PEG4000, 5 mM $MgCl_2$, 0.1 M Na-HEPES (pH 6.5), 0.2 M sodium acetate. Rod-like crystals (0.1 × 0.1 × 0.4 mm) grew within a week at 18°C. The crystals were transferred to a cryoprotectant solution containing 20% (v/v) PEG4000, 25% (v/v) glycerol, and 0.1 M Na-HEPES (pH 6.5), and flash-frozen in liquid nitrogen. Diffraction data were collected at 100 K on a single frozen crystal at the ESRF beamline ID29 (λ = 0.976 Å). Data processing and reduction were carried out using the programs MOSFLM, SCALA and TRUNCATE from the CCP4 software package (Collaborative Computational Project Number 4 1994). The crystals are monoclinic, space group $P2_1$, with cell dimensions $a = 36.54$ Å, $b = 64.91$ Å, $c = 39.77$ Å, $\beta = 110.12°$ and one enzyme monomer in the asymmetric unit. The 3D structure was determined by molecular replacement methods using the program AMoRe (Navaza 1994) and the coordinates of *B. stearothermophilus* AK (Berry and Phillips 1998; PDB code 1ZIP) as the search model. The initial Fourier difference maps revealed unambiguous electron density corresponding to the two ADP ligands. Crystallographic refinement was carried out by alternate cycles of model building with the program O (Jones et al. 1991) and refinement with the programs REFMAC5 (Murshudov et al. 1999) and ARP/wARP (Perrakis et al. 1999). The parameters after the final refinement cycles are shown in Table 1. The complete polypeptide chain is present in the model (residues

1–181), although the lateral chains of Glu22 and Arg51 are not visible due to weak electron density. According to PROCHECK (Laskowski et al. 1993), 95.6% of non-Gly and non-Pro residues lie in the most favored regions of the Ramachandran plot, while the remaining 4.4% lie in additional allowed regions. Structural superpositions of the X-ray and NMR structures were carried out using the program MASS (Dror et al. 2003). Figures 1 and 2A were prepared using PyMol v0.98 (http://pymol.sourceforge.net).

Accession number

The atomic coordinates and the structure factors have been deposited with the Protein Data Bank (PDB code 2CDN).

Acknowledgments

We thank V. Bondet and J. Bellalou (Institut Pasteur) for help with protein production. This work was partially supported by grants from the Institut Pasteur (GPH-Tuberculose), the ANRS, France (Contract No. 2003/004), the National Genopole Network (Contract RG-2002-08), and the European Commission (SPINE, Contract No. QLG2-CT-2002-00988, and X-TB, Contract No. QLK2-CT-2001-02018).

References

Andries, K., Verhasselt, P., Guillemont, J., Gohlmann, H.W., Neefs, J.M., Winkler, H., Van Gestel, J., Timmerman, P., Zhu, M., and Lee, E.2005. A diarylquinoline drug active on the ATP synthase of *Mycobacterium tuberculosis*. *Science* **307:** 223–227.

Berry, M.B. and Phillips, G.N. 1998. Crystal structures of *Bacillus stearothermophilus* adenylate kinase with bound Ap5A, Mg^{2+}Ap5A, and Mn^{2+}Ap5A reveal an intermediate lid position and six coordinate octahedral geometry for bound Mg^{2+} and Mn^{2+}. *Proteins* **32:** 276–288.

Berry, M.B., Meador, B., Bilderback, T., Liang, P., Glaser, M., and Phillips Jr., G.N. 1994. The closed conformation of a highly flexible protein: The structure of *E. coli* adenylate kinase with bound AMP and AMPPNP. *Proteins* **19:** 183–198.

Berry, M.B., Bae, E., Bilderback, T.R., Glaser, M., and Phillips Jr., G.N. 2006. Crystal structure of ADP/AMP complex of *Escherichia coli* adenylate kinase. *Proteins* **62:** 555–556.

Cole, S.T., Brosch, R., Parkhill, J., Garnier, T., Churcher, C., Harris, D., Gordon, S.V., Eiglmeier, K., Gas, S., Barry 3rd, C.E., et al. 1998. Deciphering the biology of *Mycobacterium tuberculosis* from the complete genome sequence. *Nature* **393:** 537–544.

Collaborative Computational Project Number 4. 1994. The CCP4 (Collaborative Computational Project 4) suite: Programs for protein crystallography. *Acta Crystallogr. D Biol. Crystallogr* **50:** 760–763.

Criswell, A.R., Bae, E., Stec, B., Konisky, J., and Phillips Jr., G.N. 2003. Structure of thermophilic and mesophilic adenylate kinases from the genus *Methanococcus*. *J. Mol. Biol.* **330:** 1087–1099.

Dror, O., Benyamini, H., Nussinov, R., and Wolfson, H.J. 2003. Multiple structural alignment by secondary structures: Algorithm and applications. *Protein Sci.* **12:** 2492–2507.

Gerstein, M., Schulz, G., and Chothia, C. 1993. Domain closure in adenylate kinase. Joints on either side of the two helices close like neighboring fingers. *J. Mol. Biol.* **229:** 494–501.

Jones, T.A., Zou, J.Y., Cowan, S.W., and Kjeldgaard, M. 1991. Improved methods for building protein models in electron density maps and the location of errors in these models. *Acta Crystallogr. A* **47:** 110–119.

Krishnamurthy, H., Lou, H., Kimple, A., Vieille, C., and Cukier, R.I. 2005. Associative mechanism for phosphoryl transfer: A molecular dynamics simulation of *Escherichia coli* adenylate kinase complexed with its substrates. *Proteins* **58:** 88–100.

Laskowski, R.A., MacArthur, M.W., Moss, D.S., and Thornton, J.M. 1993. Procheck: A program to check the stereochemical quality of protein structures. *J. Appl. Crystallogr.* **26:** 283–291.

Miron, S., Munier-Lehmann, H., and Craescu, C.T. 2004. Structural and dynamic studies on ligand-free adenylate kinase from *Mycobacterium tuberculosis* revealed a closed conformation that can be related to the reduced catalytic activity. *Biochemistry* **43:** 67–77.

Muller-Dieckmann, H.J. and Schulz, G.E. 1995. Substrate specificity and assembly of the catalytic center derived from two structures of ligated uridylate kinase. *J. Mol. Biol.* **246:** 522–530.

Munier-Lehmann, H., Burlacu-Miron, S., Craescu, C.T., Mantsch, H.H., and Schultz, C.P. 1999. A new subfamily of short bacterial adenylate kinase with the *Mycobacterium tuberculosis* enzyme as a model: A predictive and experimental study. *Proteins* **36:** 238–248.

Murshudov, G.N., Vagin, A.A., Lebedev, A., Wilson, K.S., and Dodson, E.J. 1999. Efficient anisotropic refinement of macromolecular structures using FFT. *Acta Crystallogr. D Biol. Crystallogr.* **55:** 247–255.

Navaza, J. 1994. AMoRe: An automated package for molecular replacement. *Acta Crystallogr. A* **50:** 157–163.

Perrakis, A., Morris, R., and Lamzin, V.S. 1999. Automated protein model building combined with iterative structure refinement. *Nat. Struct. Biol.* **6:** 458–463.

Reinstein, J., Gilles, A.M., Rose, T., Wittinghofer, A., Saint Girons, I., Barzu, O., Surewicz, W.K., and Mantsch, H.H. 1989. Structural and catalytic role of arginine 88 in *Escherichia coli* adenylate kinase as evidenced by chemical modification and site-directed mutagenesis. *J. Biol. Chem.* **264:** 8107–8112.

Reinstein, J., Schlichting, I., and Wittinghofer, A. 1990. Structurally and catalytically important residues in the phosphate binding loop of adenylate kinase of *Escherichia coli*. *Biochemistry* **29:** 7451–7459.

Rose, T., Glaser, P., Surewicz, W.K., Mantsch, H.H., Reinstein, J., Le Blay, K., Gilles, A.M., and Barzu, O. 1991. Structural and functional consequences of amino acid substitutions in the second conserved loop of *Escherichia coli* adenylate kinase. *J. Biol. Chem.* **266:** 23654–23659.

Schlichting, I. and Reinstein, J. 1997. Structures of active conformations of UMP kinase from *Dictyostelium discoideum* suggest phosphoryl transfer is associative. *Biochemistry* **36:** 9290–9296.

Sharma, K., Chopra, P., and Singh, Y. 2004. Recent advances towards identification of new drug targets for *Mycobacterium tuberculosis*. *Expert Opin. Ther. Targets* **8:** 79–93.

Sheng, X.R., Xia, L., and Xian, M.P. 1999. An iso-random Bi Bi mechanism for adenylate kinase. *J. Biol. Chem.* **274:** 22238–22242.

Yan, H. and Tsai, M.D. 1999. Nucleoside monophosphate kinases: Structure, mechanism, and substrate specificity. *Adv. Enzymol. Relat. Areas Mol. Biol.* **73:** 103–134.